

Test Method

Tracking lubricants during single screw extrusion of uPVC



J.L. Barnard, D.D. Robertson, A.J. van Reenen*

Department of Chemistry and Polymer Science, University of Stellenbosch, Private Bag XI, 7602, Matieland, South Africa

ARTICLE INFO

Keywords:

PVC
Extrusion
Lubricant
Migration
Fusion
SEM

ABSTRACT

Lubrication is one of the most important parameters in unplasticized polyvinyl chloride (uPVC) processing apart from the PVC resin and processing equipment. Lubricants are used in specific ratios to ensure effective fusion of PVC particles. The exact mechanism on how these lubricants interact is not yet fully understood. A widely accepted theory is the interaction mechanism proposed by Rabinovic et al. where lubricants are said to act as surfactants and slip agents. In this study a method for tracking lubricants, by simulating the extrusion process within a single screw extruder, was proposed. A three stage fusion simulation consisted of the feeding zone (stage 1), the compression zone (stage 2) and the metering zone (stage 3). The association interactions between the individual components of a typical uPVC formulation were followed throughout the three stages. External polar and nonpolar lubricants in combination with an internal lubricant was studied. Lubricants were successfully tracked using scanning electron microscopy coupled with energy dispersive spectroscopy (SEM-EDS). In conclusion it was found that the use of an internal lubricant promotes dispersion of external lubrication towards PVC. It was also found that there is a competition between the internal lubricant and polar external lubricant.

1. Introduction

Polyvinyl chloride (PVC) is the second most produced polymer in the world behind polyolefins [1–5]. PVC is widely used in the building industry where the primary applications include water piping and frames for doors and windows [3,5–8]. Other main consumers of PVC include the packaging and cosmetic industries [3]. Unplasticized PVC (uPVC) together with plasticised and chlorinated PVC each contribute a third of the PVC used for piping globally [9]. Production of uPVC piping is impossible without the use of various additives such as lubricants, processing aids and heat stabilizers.

According to Rabinovic et al. [10], the use of lubricants is one of the three most important parameters in uPVC processing, despite its very low concentrations within the PVC formulations. The other two parameters are the PVC resin and the processing equipment. Precisely how lubricants perform their function within these formulations has been the subject of much speculation and still has not been proven definitively.

Lubricants are generally classified as either external or internal. External lubricants are generally classified as having no chemical association with the polymer matrix. They are active at the polymer metal surface where they promote metal release and therefore delay fusion [11]. Internal lubricants are generally classified as having chemical association with both the polymer matrix as well as the external lubricant.

They are said to reduce melt viscosity and act as fusion promoter [12].

Fusion occurs when efficient friction, heat and pressure is applied to a PVC formulation. Primary PVC particles are broken down during this process allowing diffusion and entanglement of PVC chains. PVC particle surface boundaries disappear and a continuous three dimensional PVC matrix is created [13]. Efficient fusion is a very important parameter in PVC processing and is directly related to the final properties of a PVC product [14].

With regards to the processing of uPVC, various research groups have attempted to elucidate the role of lubricants during extrusion [10,11,15–17]. Rabinovic et al. investigated the lubrication mechanism by examining macroscopic properties of uPVC formulations. These measured parameters included metal release, fusion time, fusion temperature, percentage haze, changes in glass transition temperature of the PVC and rheological properties. Using transmission electron microscopy (TEM) and scanning electron microscopy (SEM), Rabinovic et al. visually interpreted how lubricants interact with the PVC matrix. Thereafter a mechanism of how internal and external lubricants should be classified as surfactants and slip agents, was proposed.

Summers et al. [12] confirmed the aforementioned mechanism by showing that lubricant failure is due to lubricant inversion from the continuous phase to a discontinuous phase with increasing melt temperatures. This was done using SEM coupled to energy dispersive x-ray

* Corresponding author.

E-mail address: ajvr@sun.ac.za (A.J. van Reenen).

spectrometry (SEM-EDS) where the Calcium (Ca) element of the Calcium stearate could visually be detected after fracturing of fused specimens. In that study Summers and co-workers used the assumption that non-polar waxes were only present in the other nonpolar areas in this system, namely the nonpolar stearate tails.

Functional waxes with characteristics of both internal and external lubricants have been the focus of more recent studies due to their effect on minimizing plate-out [1,4,5,18,19]. Plate-out occurs when additives such as stabilizers migrate out of the PVC matrix with an external lubricant. It was therefore necessary to produce an external lubricant with a slightly higher polarity which would minimise migration [19]. Examples of such lubricants include Amide and Ester based waxes [1]. It was however found that functional waxes, in addition to minimizing plate-out, exhibit advantageous properties of both internal and external lubricants. Beneficial internal lubrication properties such as shorter fusion times, lower operating pressures and torques are gained as well as comparable gloss finishes to those achieved using external waxes [19]. These functional waxes also have the added bonus of being used in much lower concentrations than when using a conventional internal/external wax combination. Until now, however, all formulations with functional waxes are still stabilized with some sort of Zn/Ca stearate internal lubrication [20].

The current study was pursued to further investigate the various mechanisms of lubricant interactions with the PVC matrix proposed in previous literature. SEM-EDS was the integral method used to track the individual components within a uPVC formulation during processing. This work gave some insight into the interactions of the individual lubricants with each other as well as the associations with the PVC matrix. A nonpolar and polar external lubricant system in combination with a Calcium stearate internal lubricant was studied.

2. Materials and methods

2.1. Materials

To investigate the mechanism at hand we selected a suitable PVC resin commercially available from Shintech (SE-950). Calcium Stearate from Chemson was selected as internal lubricant. A linear hydrocarbon wax was used as external lubricant (nonpolar). It was also decided to look at an oxidised hydrocarbon wax (polar) to investigate the effect it had on lubrication. Additives were included in excess amounts to ensure their observation during spectroscopic analysis [Table 1].

2.2. Technique

A strategy was devised to track lubricant migration using a spectroscopic technique. SEM-EDS was the principle technique of choice. It was used to visually track every component in the formula. Each component had a unique element that distinguished it from the others. For PVC this element was chloride (Cl), for calcium stearate it was the calcium (Ca), for the hydrocarbon it was the carbon (C) and for oxidised wax it was the oxygen (O).

Table 1
PVC formulations used for stage II and III.

Sample	Amounts (phr)			
	PVC	CaSt ^a	Nonpolar	Polar
a	100	–	–	–
b	100	10 and 5	–	–
c	100	–	10	–
d	100	–	–	10
e	100	10 and 5	10	–
f	100	10 and 5	–	10

^a Internal lubricant was lowered to 5 phr for stage III to minimise gas build-up within the extruder.

Tracking of these individual components was done by determining their physical positions visually at three different stages. The stages were chosen to simulate the extrusion process. Stage I was the neat characterisation of the individual components i.e. position 1. Stage II was the process of mixing at high temperatures i.e. position 2. Stage III simulated the fusion process i.e. the final position of migration.

3. Experimental

3.1. Sample preparation for all three stages

3.1.1. Stage I

Samples were characterized as is with no prior modification.

3.1.2. Stage II

Binary and ternary mixtures were hot melt blended by overhead stirring with a Heidolph RZR series mixer (2100 rpm) at 165 °C for 15 min. This temperature was chosen to ensure all the lubricants were above their melting temperatures. Mixtures and their components are listed in Table 1.

3.1.3. Stage III

For stage III the amount of calcium stearate was reduced to 5 phr to avoid gas build-up inside the extruder (Table 1*). Samples were high speed mixed with an overhead stirrer for 15 min, thereafter mixtures were subsequently extruded. Extrusion was done on a Brabender Plasticorder PLE 651 extruder with the single screw barrel attachment (L/D = 26.5:1). The barrel was preheated on three of the four sections. Section one, the feed section, was heated to 145 °C. The compression section was heated to 155 °C and the metering section was heated to 190 °C. The die area which can also be heated was removed and replaced with a short die (L/D = 5/1).

Removing this section (thus also removing the breaker plate which causes turbulent flow) caused molten polymer to maintain its directional flow. At this stage the PVC has fused and no further lubricant migration should occur. Sampling at this interval allowed for a direct interpretation of how the molten polymer matrix and the additives were interacting during directional flow. This technique is further explained in the following sections.

Approximately 9 mm diameter cross sections of the extruded material were then embedded in epoxy resin and cured in an oven at 40 °C for 24 h. Thereafter the embedded samples were polished with 9 µm (10 min), 3 µm (15 min) and 1 µm (15 min) grit polishing discs on a rotational polisher until a uniformly polished area could be observed through a light microscope.

3.2. Sample characterisation techniques

3.2.1. Stage I

Neat materials were characterized according to their molecular size, chemical composition, chain linearity and branching, and thermal behaviour using the following techniques.

3.2.2. High temperature – size exclusion chromatography (HT-SEC)

Determination of the molecular weights and molecular weight dispersity was carried out on a PL220 high temperature chromatography instrument (Polymer laboratories, Varian, Church Stretton, Shropshire, England) coupled to a differential refractive index (RI) detector. Polyethylene standards were used for calibration. Samples (4 mg) were dissolved in 1, 2, 4 – trichlorobenzene (TCB) with 0.025% butylhydroxy-toluene (BHT) stabilizer. The mobile phase had a flow rate of 1 mL/min. The stationary phase consisted of three 300 × 7.5 mm² PLgel Olexis columns (Agilent Technologies, UK) together with a 50 × 7.5 mm² PLgel Olexis guard column.

Sample volumes of 200 µL were analysed at 150 °C.

3.2.3. Attenuated total reflectance – Fourier transform infrared spectroscopy (ATRFTIR)

Analyses were carried out on a Thermo Scientific Nicolet iS10 FTIR spectrometer with a diamond crystal. Scans were performed at a resolution of 4 cm^{-1} and 64 scans were taken.

OMNIC (version 9) processing software was used for data analysis.

3.2.4. ^{13}C Nuclear magnetic resonance (^{13}C NMR)

^{13}C Nuclear magnetic resonance (^{13}C NMR) spectra were acquired on a Varian Unity INOVA 600 MHz liquid state NMR Spectrometer at $120\text{ }^\circ\text{C}$. A 90° pulse angle with acquisition time of 0.87 s and relaxation delay of 15 s was used. Detailed structural information on the waxes could be deduced from this technique.

3.2.5. Differential scanning calorimetry (DSC)

Endothermic melting and exothermic crystallization behaviour of the samples were analysed by using a TA instruments Q100 differential scanning calorimeter, calibrated with indium metal according to standard procedures. A three-step cycle was implemented wherein each sample (4 mg) was heated from room temperature to $200\text{ }^\circ\text{C}$ in the first cycle at a heating rate of $10\text{ }^\circ\text{C}\cdot\text{min}^{-1}$, this was done to remove any thermal history of the samples. Samples were kept isothermally at $200\text{ }^\circ\text{C}$ for 3 min, after which they were cooled to $25\text{ }^\circ\text{C}$ at $10\text{ }^\circ\text{C}\cdot\text{min}^{-1}$. During the final step the temperature was kept isothermally at $25\text{ }^\circ\text{C}$ for 3 min and then heated to $200\text{ }^\circ\text{C}$. Only data obtained from the second heating cycle was processed for all the thermal analysis calculations. The DSC measurements were carried out in an inert nitrogen atmosphere at a purge gas flow rate of $20\text{ mL}\cdot\text{min}^{-1}$. Data was analysed using TA universal analysis software.

3.2.5.1. Stage II and III. After undergoing their respective processes these samples were analysed using scanning electron microscopy coupled to energy dispersive X-ray spectrometry.

3.2.6. Scanning electron microscopy – Energy dispersive x-ray spectrometry (SEM-EDS)

The samples were analysed using a Zeiss EVO scanning electron microscope. Prior to imaging, the samples were mounted on aluminium stubs with double sided carbon tape. The samples were coated with a thin ($\sim 10\text{ nm}$ thick) layer of gold, using an Edwards S150A gold sputter coater. A Zeiss 5-diode back scattered electron (BSE) detector (Zeiss NTS BSD) and Zeiss Smart SEM software were used to generate BSE images. The samples were chemically quantified by semiquantitative energy dispersive x-ray spectrometry (EDS) using an Oxford Instruments® X-Max 20 mm^2 detector and Oxford Aztec software. Beam conditions during the quantitative analysis and backscattered electron image analysis on the Zeiss EVO were 20 kV accelerating voltage, 8 nA probe current, with a working distance of 8.5 mm and a beam current of 5 nA . The counting time was 10 s live-time.

4. Results and discussion

4.1. Stage I

DSC melting endotherms and crystallization exotherms are illustrated in Fig. 1a and b respectively. Both waxes exhibit melting peak maxima around $75\text{ }^\circ\text{C}$ and crystallization peak maxima around $65\text{ }^\circ\text{C}$. The waxes also exhibit bimodal thermal transitions indicating at least two different crystalline domains [21]. The main differences between the thermograms of the two lubricating waxes are the temperature ranges over which the thermal events occur. These thermal events occur over a wider temperature range for the polar wax, resulting in broader melting and crystallization distributions, whereas the nonpolar wax exhibited more homogeneous thermal profiles. This points towards differences in crystallite size distributions and chain length distribution in the two waxes. The nonpolar wax therefore has a more uniform crystal size and chain length distribution compared to that of the polar wax. The latter was further investigated using HT-SEC.

From the HT-SEC data (Table 2) it could be concluded that both

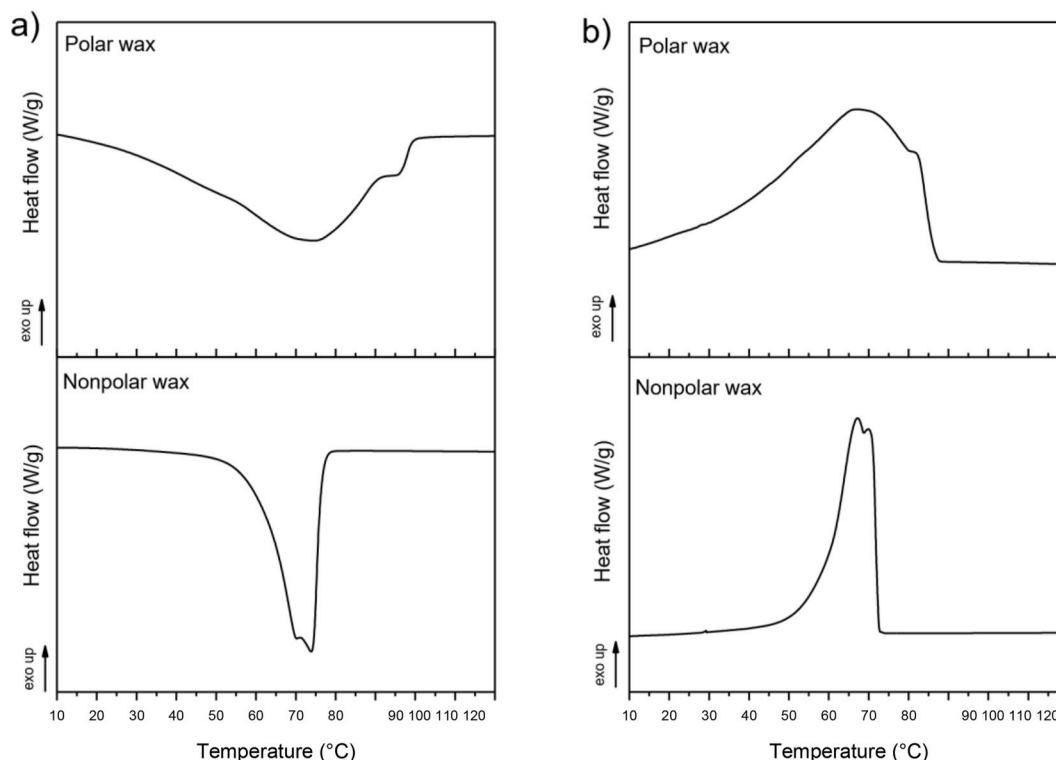


Fig. 1. DSC thermograms for polar and nonpolar waxes, a) melting endotherms and b) crystallization exotherms. Note the whole temperature profile is not shown.

Table 2

HT-SEC results for both polar and nonpolar waxes.

Wax type	M_n (g/mol)	M_w (g/mol)	M_p (g/mol)	\mathcal{D}
Nonpolar wax	298	326	307	1.2
Polar wax	267	442	354	1.7

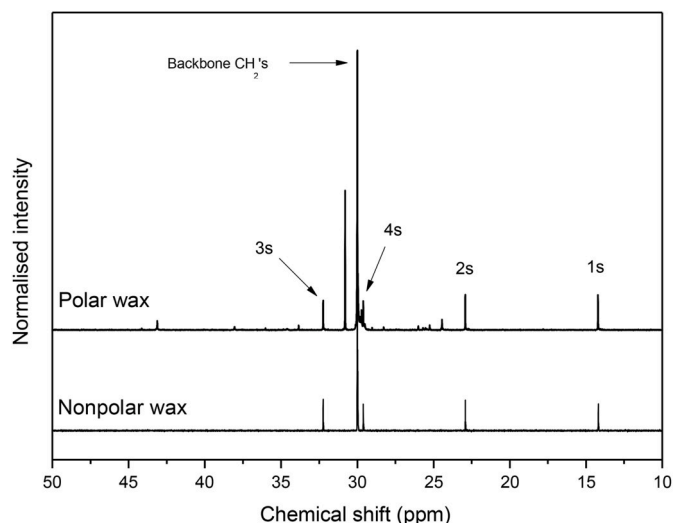
waxes have similar molecular sizes (hydrodynamic volumes), $M_n \approx 300$ g/mol. However, the molecular weight distribution or molecular weight dispersity (\mathcal{D}) for the nonpolar wax was noticeably lower compared to the polar counterpart. These results were in good correlation with the conclusions drawn from the DSC data, with a larger molecular weight dispersity resulting in broader thermal transition distribution for the polar wax.

Chemical composition was investigated by ATR-FTIR. Fig. 2 shows the ATR-FTIR spectra of both waxes. Both spectra showed distinct methyl and methylene stretching as well as methylene bending vibrations around 2900 cm^{-1} , 1460 cm^{-1} and 720 cm^{-1} respectively. These vibrational bands are indicative of a predominantly hydrocarbon-based backbone structure. The polar oxidised sample however clearly showed signs of oxygenated moieties evident by the presence of bands at 3480 cm^{-1} , 1720 cm^{-1} and 1170 cm^{-1} attributed to O-H, C=O and C-O stretching vibrations.

Molecular chain linearity of the waxes was probed by ^{13}C NMR. Spectra are illustrated in Fig. 3. The spectra of the nonpolar wax was characteristic of a highly linear hydrocarbon with only signals arising from the chain end carbons (1s, 2s, 3s and 4s) and backbone methylene carbons. The extra signals observed in the spectra of the polar wax were due to carbons in the vicinity of oxygenated moieties along the molecular backbone (e.g. peaks at 43 ppm and 24 ppm represents the carbons in α and β position to carbonyl groups). No clear evidence of chain branching were detected. From NMR and FTIR it could be concluded that both wax samples were predominantly linear with the major difference being the presence of polar oxygenate moieties within the polar wax sample.

4.2. Stage II

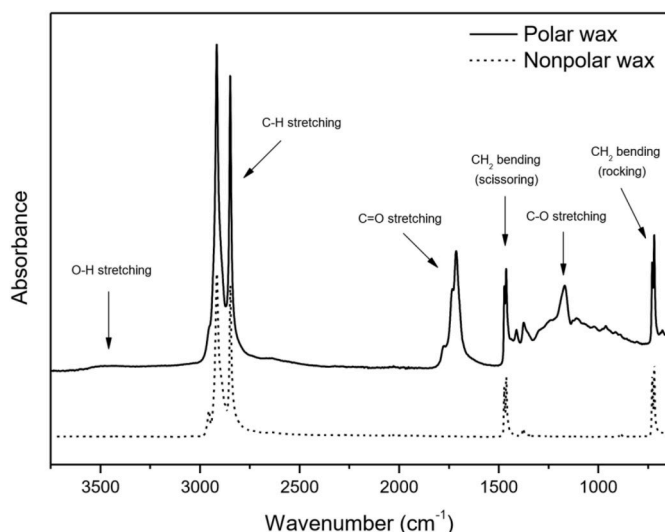
Fig. 4 illustrates the electron images and SEM-EDS signals of the neat PVC particles and blended PVC particles after high speed melt mixing with internal and external lubricants. The neat PVC particle surface appeared to be uneven and showed visible crevices. These crevices contribute to the sample's porosity [22]. A strong uninterrupted chloride (Cl) signal was observed from SEM-EDS measurements which

**Fig. 3.** ^{13}C NMR spectra for both waxes.

corresponds perfectly with the electron image of the neat PVC particle. Addition of the CaSt as internal lubricant clearly decreased the Cl signals implying the partial coverage of the PVC particles with CaSt. It shows crevices being occupied by the internal lubricant to some extent, which might indicate physical or chemical association between polymer and internal lubricant. This is clearly visible in Fig. 4b where the blue chloride signals are interrupted. The carbon signals are also intensified due to the presence of the aliphatic carbon chain of the stearate moiety in the CaSt molecule. Furthermore, the presence of the internal lubricant on the PVC was confirmed by the characteristic SEM-EDS oxygen (O) and calcium (Ca) signals. Physical association between lubricant and PVC could possibly occur due to the crevices allowing entrapment of lubricant molecules or possible chemical association could be facilitated through the polar groups of the stearate moiety of the CaSt with the PVC.

Clear differences could be seen with addition of the two respective waxes. The nonpolar wax tended to accumulate within the uneven crevices of the PVC particles, whereas the polar wax had a tendency to cover a larger area across the smooth surface of the particles. This is visually represented by Fig. 4c where the Cl signals are very similar to the neat PVC profile, apart from the darker regions within the crevices due to nonpolar wax accumulations. A more uniform decrease in Cl signals can be seen in Fig. 4d due to covering of the particle by the more polar wax. Higher carbon signal intensities and uniform oxygen signals further confirmed the enhanced coating of the PVC particle with the more polar external lubricant. This could be indicative of a greater affinity of the polar external lubricant for PVC compared to the nonpolar counterpart.

Fig. 4e and f represents the ternary blends where the PVC was mixed with both the external and internal lubricants. A distinct decrease in Cl signal intensity together with a stronger carbon signal was observed in Fig. 4e when compared to its binary counterpart in Fig. 4c. The lubricant coverage is also visible from the electron image. The carbon signals are also closely associated with the calcium signals, indicating possible interaction between the internal and external lubricants. Homogeneous carbon, oxygen and calcium signals across the PVC surface point towards the compatibilization of nonpolar external lubricant with the PVC particles through addition of the internal CaSt lubricant. These enhanced associations are most probably facilitated through nonpolar interactions between the aliphatic stearate tails of CaSt with the aliphatic chains of the nonpolar lubricant, and through polar interactions between the polar stearate heads with the polar PVC surface. Particle coverage for the ternary blend containing nonpolar wax appeared to be greater and more homogeneous compared to the binary PVC/nonpolar wax blend.

**Fig. 2.** ATR-FTIR spectra for both waxes.

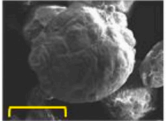

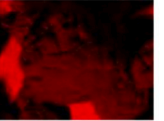
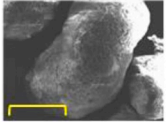
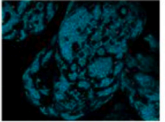
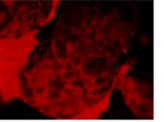
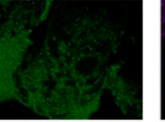
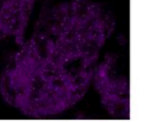
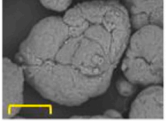
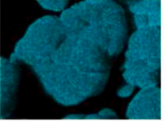
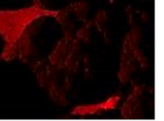
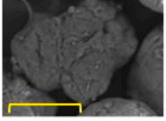
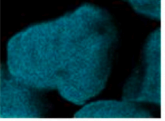
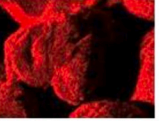
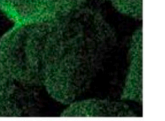

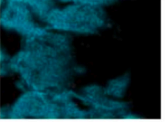
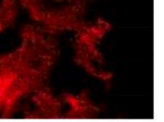
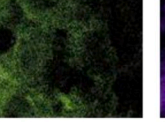
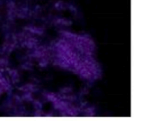
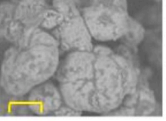

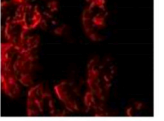

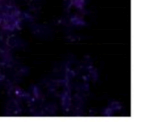
Stage II		Element ($k\alpha$)				
Sample	Electron Image	Cl	C	O	Ca	
a						
b						
c						
d						
e						
f						

Fig. 4. SEM electron images and SEM-EDS elemental signal maps for neat PVC and PVC/Lubricant blends: a) neat PVC; b) PVC/CaSt; c) PVC/nonpolar wax; d) PVC/polar wax; e) PVC/CaSt/nonpolar wax; f) PVC/CaSt/polar wax. Scale bar = 100 μm .

Conversely, the particle coverage of the ternary blend containing the polar external lubricant were not as homogeneous across the PVC surface. From the electron image in Fig. 4f the lubricants appeared to accumulate mainly in the crevices. This phenomena could be due to competition between the polar groups of the internal lubricant and the polar wax. The internal lubricant did not promote the particle coverage as in the case of the nonpolar ternary blend and was confirmed by the lower signals for C/O/Ca on the particle surfaces. It should be noted at this stage that images 4b and 4f show similar association behaviour towards the PVC particles.

At this point it could be concluded that the internal lubricant facilitated associations and particle coverage when the nonpolar wax was used. However, when the polar wax and internal lubricant was used the particle coverage was somehow hindered. When using the polar lubricant in the absence of the CaSt, a much better uniform particle coverage was observed. The next step was to put the blends through an extrusion cycle and study distribution and migration of these lubricants within the different formulations.

4.3. Stage III

The extruded blends (stage III), illustrated by Fig. 5, showed the development of some interesting morphologies. As the polymer mixture exits the extruder, the fused sample seems to fold onto itself, resulting in a spiral morphology. This provided an indication of what is really

happening within the barrel. In the case of PVC research this hasn't as yet been reported to a great extent.

Fig. 5a illustrates dominant Cl signals (EDS signal) due to the neat PVC composition as well as a smooth homogeneous morphology as seen from the electron image. The carbon signal observed towards the middle of the sample arise from residual polyethylene cleaning agent used to purge the barrel in-between batches. In Fig. 5b an enhanced spiralling effect can be observed. The morphology was also highly phase separated with distinct polar (Cl) and nonpolar wax (C) regions. This is an indication of poor association between the internal lubricant and the PVC within this binary blend.

Interestingly, when analysing the binary blends which only consist of the external lubricants and PVC (Fig. 5c and d), homogeneous distributions of the Cl and C signals were observed. In the presence of the oxidised polar lubricant, the oxygen signals were also homogeneously spread throughout the sample. Visual observations from Fig. 5b–d clearly points towards differences in associations of the external and internal lubricants towards the PVC.

When comparing the two ternary blends in Fig. 5e and f, completely different morphologies were observed. In the presence of nonpolar wax a smooth uniform morphology was seen with homogenous distribution of all elemental signals. In this case it is possible that the nonpolar lubricant functioned as a compatibilizer and promoted improved distribution of the internal lubricant and far less phase separation is visible compare to Fig. 5b. However, in the presence of polar wax, the ternary

Stage III		Element ($k\alpha$)			
Sample	Electron Image	Cl	C	O	Ca
a					
b					
c					
d					
e					
f					

Fig. 5. SEM electron images and SEM-EDS elemental signal maps for neat PVC and PVC/Lubricant blends: a) neat PVC; b) PVC/CaSt; c) PVC/nonpolar wax; d) PVC/polar wax; e) PVC/CaSt/nonpolar wax; f) PVC/CaSt/polar wax. Scale bar = 3 μ m.

blend showed a phase separated morphology worse than its binary PVC: CaSt and PVC:polar wax counterparts. This observation was consistent with the differences in coverage of the PVC particles illustrated and discussed previously in Fig. 4. It can thus be concluded that some degree of competition in the affinity for the PVC exist between the internal lubricant and the polar external lubricant when used together and hence the clear phase separated morphology.

5. Conclusion

Three stages of lubricant migration during PVC processing was investigated. In stage one the materials were characterized according to size, chemical composition, chain linearity/branching and thermal behaviour.

Stage two was set up to represent the compression section on a typical single screw extruder. Here, insight into how the individual components would associate be it chemically or physically, were obtained. It was seen that nonpolar waxes had no affinity for PVC on its own and oxidised wax exhibited some association. Addition of calcium stearate to the system facilitated association of nonpolar wax to the PVC and less so for polar wax. The polar wax showed a competition effect and seemed to rather associate with CaSt than PVC.

Stage 3 represented PVC fusion during the metering stage on the extruder. Two phases were identified during this stage namely a polar

PVC phase and a nonpolar hydrocarbon phase. Focus was placed on the polar PVC areas and how well the lubricants were dispersed within it. The polar wax had a better dispersion in the PVC matrix compared to the nonpolar wax. Upon addition of CaSt the nonpolar wax had a similar distribution pattern to its binary blend within the PVC matrix. Addition of both CaSt and polar wax to the formulation resulted in a completely phase separated distribution.

In accordance with the surfactant/slip-agent theory, the internal and external lubricants showed a definite affinity for each other. The nonpolar wax did not associate with PVC by itself but only in the presence of CaSt, proving that the nonpolar wax only associates with the nonpolar aliphatic tails of CaSt. No evidence was found to suggest the CaSt creates a boundary layer on the metal– polymer or in between the PVC–wax interface. We suggest further on-line monitoring of the migration event.

Data availability

The raw/processed data required to reproduce these findings cannot be shared at this time due to technical or time limitations.

Declaration of competing interest

The authors declare that they have no known competing financial

interests or personal relationships that could have appeared to influence the work reported in this paper.

CRedit authorship contribution statement

J.L. Barnard: Methodology, Investigation, Writing - original draft.
D.D. Robertson: Supervision, Writing - review & editing. **A.J. van Reenen:** Conceptualization, Supervision, Writing - review & editing.

Acknowledgments

The authors would like to thank the staff of the SEM unit at the Central Analytical Facility (CAF) at Stellenbosch University for assistance with the SEM-EDS analyses.

This research did not receive any specific grant from funding agencies in the public, commercial, or not-for-profit sectors.

Appendix A. Supplementary data

Supplementary data to this article can be found online at <https://doi.org/10.1016/j.polymertesting.2020.106523>.

References

- [1] M. Gilbert, S. Patrick, Poly(Vinyl Chloride), Elsevier Ltd, 2016, <https://doi.org/10.1016/B978-0-323-35824-8.00013-X>.
- [2] N.A. Mohamed, Antimicrobial itaconimido aromatic hydrazide derivatives for inhibition of the thermal degradation of rigid PVC, *Polym. Bull.* 76 (2019) 2341–2365, <https://doi.org/10.1007/s00289-018-2486-8>.
- [3] M.H. Al-Malack, Migration of lead from unplasticized polyvinyl chloride pipes, *J. Hazard Mater.* 82 (2001) 263–274, [https://doi.org/10.1016/S0304-3894\(00\)00366-6](https://doi.org/10.1016/S0304-3894(00)00366-6).
- [4] S. Coomans, Development and Evaluation of an Acrylic Lubricant for PVC Formulations, MSc Thesis, Hasselt University, 2017.
- [5] S. Moore, Global Trends in PVC Resin Applications and Additives Usage, Townsend solutions, 2018. http://www.vinyl.org.au/images/vinyl/Events/PVCAUS2018presentations/Stephen-Moore_Townsend-r1.pdf.
- [6] S. Jeon, K.-T. Kim, K. Choi, Migration of DEHP and DINP into dust from PVC flooring products at different surface temperature, *Sci. Total Environ.* 547 (2016) 441–446, <https://doi.org/10.1016/j.scitotenv.2015.12.135>.
- [7] T. Maes, R. Jessop, N. Wellner, K. Haupt, A.G. Mayes, A rapid-screening approach to detect and quantify microplastics based on fluorescent tagging with Nile Red, *Sci. Rep.* 7 (2017), 44501, <https://doi.org/10.1038/srep44501>.
- [8] F. Mao, Permeation of Hydrocarbons through Polyvinyl Chloride (PVC) and Polyethylene (PE) Pipes and Pipe Gaskets, PhD Thesis, Iowa state University, 2008, <http://lib.dr.iastate.edu/rtd>. (Accessed 9 March 2018).
- [9] S.S. Yashwant, PVC pipe market, *Market. Res. Rep.* (2019) 157. <https://www.alliedmarketresearch.com/pvc-pipes-market/>. (Accessed 9 October 2019).
- [10] E.B. Rabinovitch, E. Lacatus, J.W. Summers, The lubrication mechanism of calcium stearate/paraffin wax systems in PVC compounds, *J. Vinyl Addit. Technol.* 6 (1984) 98–103, <https://doi.org/10.1002/vnl.730060303>.
- [11] L.F. King, F. Noel, Characterization of lubricants for polyvinyl chloride, *Polym. Eng. Sci.* 12 (1972) 112–119, <https://doi.org/10.1002/pen.760120207>.
- [12] J.W. Summers, Lubrication mechanism of poly(vinyl chloride) compounds: changes upon PVC fusion (gelation), *J. Vinyl Addit. Technol.* 11 (2005) 57–62, <https://doi.org/10.1002/vnl.20037>.
- [13] M.A.M. Moghri, H. Garmabi, Effects of additives on fusion parameters of rigid PVC formulations, *J. Vinyl Addit. Technol.* 21 (2008) 129–133, <https://doi.org/10.1002/vnl>.
- [14] J. Tomaszewska, T. Sterzynski, K. Piszczek, Rigid poly(vinyl chloride) (PVC) gelation in the brabender measuring mixer. I. Equilibrium state between sliding, breaking, and gelation of PVC, *J. Appl. Polym. Sci.* 93 (2004) 966–971, <https://doi.org/10.1002/app.20519>.
- [15] C.I. Chung, W.J. Hennessey, M.H. Tusim, Frictional behavior of solid polymers on a metal surface at processing conditions, *Polym. Eng. Sci.* 17 (1977) 9–20, <https://doi.org/10.1002/pen.760170103>.
- [16] T.C. Pedersen, Process and material considerations in the industrial application of lubricants in rigid PVC extrusion, *J. Vinyl Technol.* 6 (1984) 104–109, <https://doi.org/10.1002/vnl.730060304>.
- [17] M. Fisch, R. Bacaloglu, Study of additive compatibility with poly(vinyl chloride) (PVC). 2: dynamic mechanical analysis of PVC lubrication by stearic acid and its derivatives, *J. Vinyl Addit. Technol.* 4 (1998) 4–11, <https://doi.org/10.1002/vnl.10002>.
- [18] N. Varshney, M. Gilbert, M. Walon, S. Michael, Plate-out in PVC extrusion. II. Lubricant effects on the formation of die plate-out in lead-based rigid PVC formulations, *J. Vinyl Addit. Technol.* 18 (2012) 209–215, <https://doi.org/10.1002/vnl>.
- [19] B. Treffler, Impact of lubricants on processing behaviour of U-PVC, *Plast. Rubber Compos.* 34 (2005) 143–147, <https://doi.org/10.1179/174328905X55506>.
- [20] R. Spiekermann, New lubricants offer higher efficiency in PVC extrusion, *Plastics, Addit. Compd.* 10 (2008), [https://doi.org/10.1016/S1464-391X\(08\)70173-9](https://doi.org/10.1016/S1464-391X(08)70173-9).
- [21] G. Webber, The Origin of Multiple DSC Melting Peaks of Fischer-Tropsch Hard Waxes, PhD Thesis, University of Cape Town, 2009.
- [22] J.F.J. Coelho, A.C. Fonseca, P.M.F.O. Gonçalves, A.V. Popov, M.H. Gil, Particle features and morphology of poly(vinyl chloride) prepared by living radical polymerisation in aqueous media. Insight about particle formation mechanism, *Polymer (Guildf)* 52 (2011) 2998–3010, <https://doi.org/10.1016/j.polymer.2011.05.014>.